Solar-Terrestrial Physics. 2025, vol. 11, iss. 4, pp. 83–96. DOI: 10.12737/stp-114202509. © 2025 A.Yu. Gvozdarev, E.O. Uchaikin. Published by INFRA-M Academic Publishing House

DOI: 10.12737/stp-114202509

Received October 01, 2024
Accepted May 13, 2025

EXPERIENCE IN MONITORING GEOMAGNETICALLY INDUCED CURRENTS IN THE ALTAI REPUBLIC POWER GRID

A.Yu. Gvozdarev
Institute of Cosmophysical Research and Radio Wave Propagation FEB RAS, Paratunka, Russia, gvozdarev@ikir.ru

E.O. Uchaikin
Gorno-Altaisk State University, Gorno-Altaisk, Russia, evgeniy_uch@mail.ru

Abstract. A device for measuring geomagnetically induced currents (GICs) has been created which is installed at the Ininskaya power substation in the Altai Republic. Since April 2024, periodic monitoring of GIC in the 110 kV power transformer grounding neutral has been carried out. GICs were registered during geomagnetic disturbances up to 138 mA, which, taking into account the parallel grounding of the Ininskaya substation and the Ininskaya solar power plant, means the presence of 1.3 A total GIC in the grounding of both objects. GICs are shown to occur during Pc3 and Pc5 geomagnetic pulsation observations. The qualitative agreement has been found between the GIC measurement results and the model values calculated from Baigazan magnetic station data in the approximation of the homogeneous Earth's crust conductivity. The grounding resistance is shown to exert an effect on recorded GICs.

Keywords: geomagnetically induced currents, monitoring, simulation, geomagnetic storms, geomagnetic pulsation, Gorny Altai.

INTRODUCTION

Geomagnetically induced currents (GICs) are a potentially dangerous phenomenon of space weather. During strong variations in the geomagnetic field (GMF), a geoelectric field arises in the conductive Earth crust due to electromagnetic induction. This field (and its associated electromotive force) generates GICs flowing in high-voltage power transmission lines (PTL) between grounding points of power transformers. Passing through primary windings of transformers, GICs produce a quasi-direct magnetic field in their cores, which leads to a decrease in the efficiency of transformers, the generation of even harmonics, an increase in reactive power, phase asymmetry, and incorrect operation of automation [Pilipenko, 2021]. The GIC magnitude depends on the geomagnetic latitude (they are more intense in the auroral zone, up to 300 A), and the electrical resistivity (ER) of underlying rocks (above a high-resistance foundation of crystalline rocks, GICs are higher), PTL length, topology, and orientation, as well as resistance of PTL, high voltage windings of transformers and their groundings. The effect of GICs on transformers depends on the design of their magnetic circuits and the magnitude of open-circuit current. For high-voltage transformers (500 kV), incorrect operation of automation due to magnetic circuit saturation is possible already at GIC ~4 A [Gusev et al., 2020]. The power failures caused by GICs in Quebec (Canada) on March 13–14, 1989 [Bolduc, 2002] and in Southern Sweden in November 2003 [Pulkkinen et al., 2005] are widely known.

In recent years, a significant number of papers have been published which deal with GICs in power grids at middle and low latitudes [Pilipenko, 2021; Gil et al., 2023]. There have been reports on failures in generator step-up transformers at a number of large power plants in South Africa due to a series of magnetic storms in 2003 [Gaunt, Coetzee, 2007] and on power accidents in New Zealand [Marshall et al., 2013]. There were sharp variations in reactive power on 400 kV PTL during magnetic storms in southern countries such as Zimbabwe [Muchini et al., 2024] and Iran [Taran et al., 2023]. Modeling has shown that a power failure can occur in the European part of Russia during an extreme storm [Tren'kin et al., 2023]. Sokolova et al. [2019] report possible instability of the Siberian energy system to GICs. All this shows the relevance of research into GICs at midlatitudes, in particular in Siberia.

At middle and low latitudes, GIC monitoring systems have been created in New Zealand [Mac Manus et al., 2017], Brazil [Trivedi et al., 2007], Austria [Albert et al., 2021], China [Zhang et al., 2015], Japan [Watari et al., 2021], Great Britain [Hubert et al., 2024], Spain [Marsal et al., 2021], Mexico [Caraballo et al., 2023]; GICs are reported to be up to 113 A in New Zealand [Mac Manus et al., 2025], up to 30 A in the United Kingdom [Hubert et al., 2024], up to 14 A in Austria [Bailey et al., 2022], up to 15 A in Brazil [Trivedi et al., 2007]. Significant efforts have been made to simulate GICs at middle and low latitudes [Švanda et al., 2021; Barbosa et al., 2015; Espinosa et al., 2023; Hubert et al., 2024; Matandirotya et al., 2015; Caraballo et al., 2023] and to predict their magnitudes [Bailey et al., 2022].

In Russia, GICs are recorded only at substations of the Northern Transit 330 kV main transmission line on the Kola Peninsula and in Karelia, i.e. in polar and circumpolar latitudes [Selivanov et al., 2023]. Since 2011, we have collected significant material; at the power substation Vykhodnoy, GICs up to 94 A in a transform-

This is an open access article under the CC BY-NC-ND license

er were recorded (up to 125 A when the grid configuration was changed).

At midlatitudes of Russia, no direct measurements of GICs were carried out; however, by indirect methods (based on the presence of even harmonics in the grid), the GIC effect on power systems of Kamchatka [Sivokon, 2021] and Altai [Uchaikin, Gvozdarev, 2023] was detected. We have attempted to organize the monitoring of GIC in the 110 kV power grid of the Altai Republic. In this paper, we describe this work and its initial results.

For further analysis, it is worthwhile making general estimates of GIC magnitude at midlatitudes. GICs are a manifestation of the skin effect [Parkinson, 1986]. During variations in the geomagnetic field **B**, a geoelectric field **E** is generated in the Earth's crust, which depends on the rate of change of the geomagnetic field. In the approximation of smallness of the displacement current density, Maxwell equations for a conducting medium with a specific conductivity σ can be written as

$$\mathrm{rot}\,\mathbf{E} = -\frac{\partial \mathbf{B}}{\partial t}, \tag{1.1}$$

$$\mathrm{rot}\,\mathbf{B} = \mu_0 \sigma \mathbf{E}, \tag{1.2}$$

where $\mu_0 = 4\pi \cdot 10^{-7}$ H/m is the magnetic constant. In the event of homogeneous conductivity for a magnetic field varying according to the harmonic law (on the Earth surface) $\mathbf{B} = \mathbf{B}_0 e^{i\omega t}$, the solution of these equations is a wave exponentially decreasing with depth $\mathbf{E} = \mathbf{E}_0 e^{-z/h} e^{i(\omega t - z/h)}$ [Parkinson, 1986]; in this case, electric and magnetic field vectors are mutually orthogonal and horizontally oriented. Depth of penetration of vortex geoelectric and alternating magnetic fields (thickness of the skin layer)

$$h = \sqrt{2\rho/(\omega\mu_0)} \tag{2}$$

depends on electrical resistivity (ER) of underlying rocks $\rho = 1/\sigma$ and the cyclic frequency of field oscillations ω. For example, h=113 km at ρ=500 Ω·m and 100 s period of magnetic variations. As is seen from Formula (2), with an increase in ER and in the oscillation period, the depth of penetration of the electromagnetic field increases; therefore, in mountainous areas GIC is generated more effectively. The difference between average ER of upper 10 km of the geoelectric cross-section in Russia is several orders of magnitude: from ~1 Ω·m in the Caspian Lowland to hundreds of kΩ m in Karelia and on the Kola Peninsula. The mountain systems of Southern Siberia are characterized by ER ~1–10 kΩ·m [Kozyreva et al., 2022, Alekseev et al., 2015]. In reality, the situation is complicated by the heterogeneity of the geoelectric cross-section, so the formulas presented above can only be considered as simplified estimates.

The vortex geoelectric field resulting from electromagnetic induction during geomagnetic field variations creates an electromotive force applied to grounding points of the power grid, which generates quasi-direct GIC at them with frequencies from fractions of mHz to 1 Hz (Figure 1). For example, given the rate of change of the magnetic field dB/dt=0.5 nT/s (this value was taken as threshold for the GIC effect on the Siberian power system in [Vodyannikov et al., 2006]), the distance between grounding points L=100 km, and the depth of field penetration h=100 km according to the law of electromagnetic induction, the electromotive force can be estimated as

$$\varepsilon = \left|\frac{dB}{dt}\right| hL = 0.5 \cdot 10^{-9}\ \frac{\mathrm{T}}{\mathrm{s}} \cdot 10^5\ \mathrm{m} \cdot 10^5\ \mathrm{m} = 5\ \mathrm{V}.$$

This suggests that the thickness of the skin layer h plays an essential role in GIC magnitude: along with the distance between grounding points L, it determines the cross-section area through which the alternating magnetic flux passes (marked with the rectangle in Figure 1). The resulting voltage between the grounding points produces a current through PTL, whose magnitude depends on the resistance of the circuit comprising PTL, high-voltage windings of power transformers, and neutral grounding of transformers. With resistances of the order of 10 Ω in 110 kV PTL, we can expect GIC ~0.5 A.

1. FEATURES OF THE 110 kV POWER GRID OF THE ALTAI REPUBLIC

The choice of the region for the research was dictated by the presence of the Baigazan magnetic station of Gorno-Altaisk State University, which has been monitoring geomagnetic variations since 2009, on the territory of the Altaiskiy Nature Reserve [Bakiyanov et al., 2011]. The station operates a quartz variometer with a recording frequency of 20 Hz and a noise amplitude (standard deviation of averages per second) 0.01–0.03 nT. The distance from the station to substations of the 110 kV power grid in the Altai Republic does not exceed 200 km, which allows a relatively accurate estimate of GIC in it through simulation [Gvozdarev et al., 2023; Uchaikin et al., 2024].

The personal factor also played an important role — one of the authors of the paper has skills as both a developer of geophysical equipment and an energy expert. To simply enter the territory of a high-voltage substation,

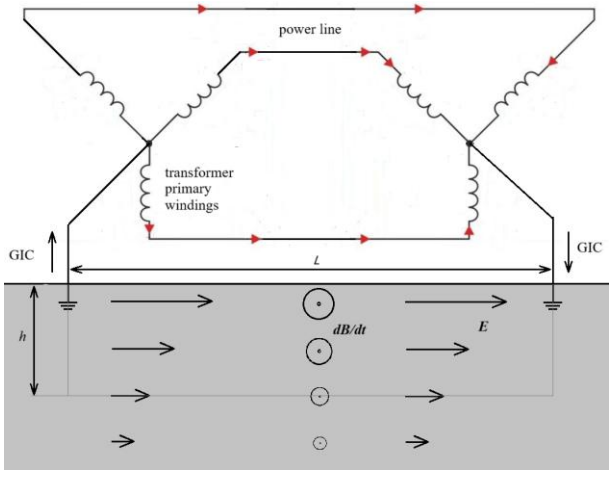

Figure 1. GIC generating circuit

it is necessary to have an electrical safety permit for voltages of 1000 volts or more, whereas geophysicists usually do not have it. This difficulty is avoided in different ways, for example, by measuring GIC outside substations, using differential magnetometry methods, as researchers in Namibia [Matandirotya et al., 2016], Great Britain [Hubert et al., 2024] and Spain [Marsal et al., 2021] have done, or by measuring VLF emission from PTL as in Kamchatka [Sivokon, 2021].

In the Altai Republic, as in a number of sparsely populated regions, a 110 kV power grid more than 500 km long is employed to supply electricity. This voltage, which is commonly used in industrialized regions for a district grid, has been chosen because the energy consumption in villages is low (to 40 MW). For safe operation, the neutral grounding circuit for 110 kV power transformers with special grounding device switches is adopted; therefore, the line is grounded at the ends and at some intermediate substations. The large length of the Altai Republic power system makes it relatively susceptible to magnetic storms.

The scheme of the central and southern parts of the 110 kV power grid of the Altai Republic is given in Figure 2. Stars mark the points for recording geomagnetic variations at the Baygazan station [Bakiyanov et al., 2011], on Lake Teletskoye, geomagnetically induced currents and amplitudes of even harmonics [Uchaikin, Gvozdarev, 2023] at the Ininskaya power substation. The scheme also shows solar power plants (SPPs) of regional importance. The main transmission of power is carried out via 110 kV PTL from Biysk TPP, located more than 70 km to the north outside the circuit. Power transformer neutrals are grounded at substations in Kosh-Agach, Ulagan, Inya, Cherga, Ust-Koksa, as well as at the Ininskaya SPP.

It has been shown [Uchaikin, Gvozdarev, 2023] that during geomagnetic disturbances, the amplitudes of the fourth and sixth harmonics of the transformer magnetic field at the Ininskaya power substation are proportional to the square of the rate of change of the magnetic field horizontal component dB/dt, which indicates its susceptibility to GIC [Uchaikin et al., 2025]. In this regard, it was decided to install a GIC measuring device at the Ininskaya power substation. Referring to Figure 2, GIC in Inya is actually the sum of three currents generated in the Inya–Kosh-Agach, Inya–Ulagan, and Inya–Cherga PTLs. The first two PTLs have a predominantly latitudinal direction. According to modeling [Gvozdarev et al., 2023; Uchaikin et al., 2024], GICs are usually generated in the PTLs during a rapid change of the GMF northward component, typical, for example, of storm sudden commencements (SSCs). The Cherga–Inya PTL has a large section mainly along the meridian; therefore, GIC in it also appears when the GMF eastward component changes. Since all these GICs are not balanced, they will be recorded at the Ininskaya power substation in case of any changes in the geomagnetic field. Preliminary estimates through modeling have shown that GICs to 0.4 A can occur in the Altai Republic high-voltage power grid [Uchaikin et al., 2024]. Thus, the measuring complex should have a resolution of tens, and preferably a few milliamper.

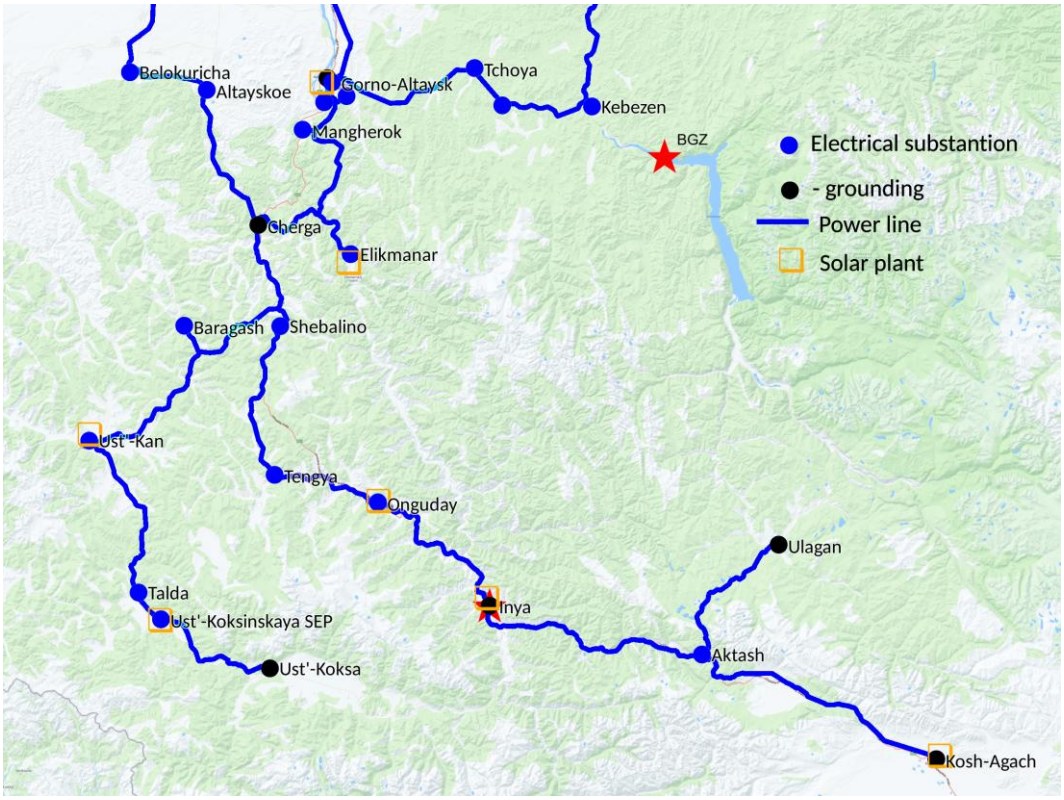

Figure 2. Scheme of the 110 kV power grid in the central and southern regions of the Altai Republic. Stars indicate the location of monitoring points of geomagnetic variations (BGZ) and the amplitude of even harmonics of alternating current and GIC in the Altai Republic power grid

2. DEVELOPMENT OF MEASURING COMPLEX

To ensure monitoring of continuous neutral current measurements, a measuring complex has been developed from modified standard clamp-type current sensor using Hall element for measuring direct current. In addition, a temperature sensor was installed for subsequent temperature correction. The voltage output is measured by the developed voltage recorder based on a precision 24-bit 2-channel ADC AD7732 by recording the measuring time (UTC) with a GPS module and measured data to an SD card. The measurement is performed in two channels with a frequency of 100 Hz. The ADC intrinsic noise does not exceed 20 μV at a range ±10 V. The sensitivity of the current clamps was increased from 10 to 22 mV/A. The sensitivity was determined using the AC power supply AKIP-1102 in the range ±3 A. The recording equipment of the complex was developed from an induction magnetometer installed at the Baigazan magnetic station [Uchaikin et al., 2015].

To balance the temperature dependence, a series of measurements of zero current was carried out at varying temperatures under natural conditions in a temperature range from –10 to 30 °C. Figure 3, *a* shows that with increasing temperature the slope coefficient decreases and the temperature dependence is nonlinear. The temperature dependence was approximated by a third degree polynomial:

$$I_{base}(T) = -8.3\cdot10^{-5}T^3 + 5.59\cdot10^{-3}\cdot T^2 - \\ -0.1855\cdot T + 2.07,$$

where T is the temperature.

The distribution of the number of measurements carried out for 15 min at zero current is illustrated in Figure 3, *b*. The distribution is normal with a standard deviation (SD) of 0.5 mA. According to the three sigma rule, the confidence interval of the measuring complex is ±1.5 mA.

To minimize rapid temperature changes, the sensor was placed in a thermobox. Analysis of the measurement results has shown that the thermal inertia of the thermobox made it possible to avoid temperature fluctuations with a period less than 15 min.

The use of the 24-bit ADC in the measuring complex allowed us to obtain a fairly wide dynamic measurement range: about ±450 A with a sampling step ~0.05 mA and an intrinsic noise ~0.5 mA. For example, the measuring system exploited on the Kola Peninsula employs an 11-bit ADC, with a measurement limit ±125 A at the substation Vykhodnoy and ±62.5 A at other substations with a sampling step of 0.12 and 0.06 A respectively [Barannik et al., 2012].

However, one of the key parameters in GIC recording systems with Hall sensors is temperature stability. On the Kola Peninsula, the recording is made by current clamps located in a thermostabilized box (the accuracy of temperature control is 0.1 °C), which allows for a very small (compared with our measurements) zero drift during the day [Barannik et al., 2012].

3. ORGANIZATION OF CURRENT MONITORING IN THE POWER TRANSFORMER NEUTRAL AT THE ININSKAYA SUBSTATION

On April 15, 2024, the measuring complex was installed in the 110/10 kV Ininskaya power substation in the T1 2.5 MVA transformer neutral, under which a recorder of even harmonics had previously been installed [Uchaikin, Gvozdarev, 2023]. The position of elements of the measuring complex is illustrated in Figure 4, which shows the data logger, the current clamps, and the neutral grounding bus. To obtain an even temperature distribution and minimize heating, the current clamps were placed in a thermobox. The photo also shows the sensor of the recorder of even harmonics under the power transformer.

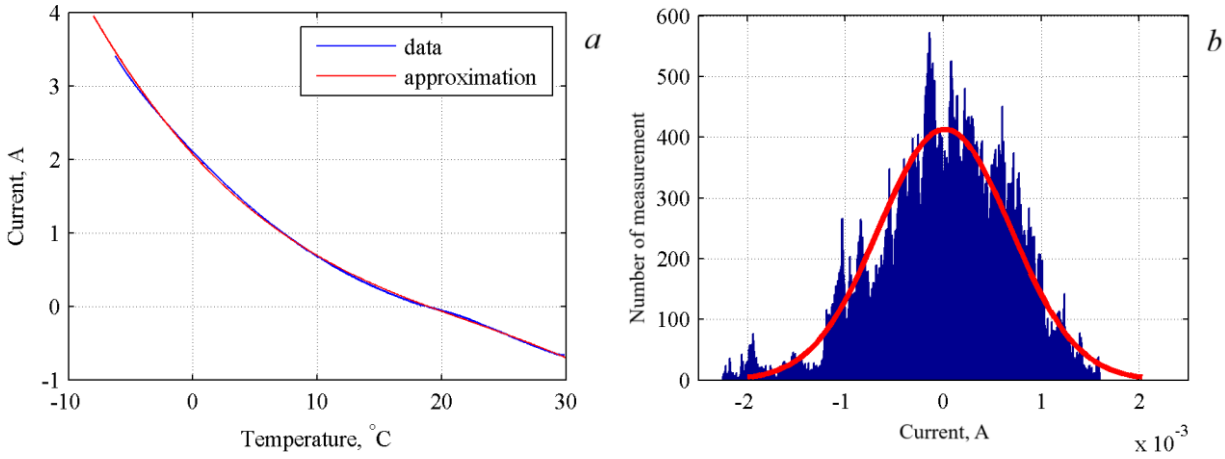

Figure 3. Results of studies on the temperature dependence of readings of modified current clamps and estimation of their noise: the dependence of measured values at zero current through the clamps under changes of temperature (*a*); distribution of measurement error at zero current for 15 min at constant temperature (*b*)

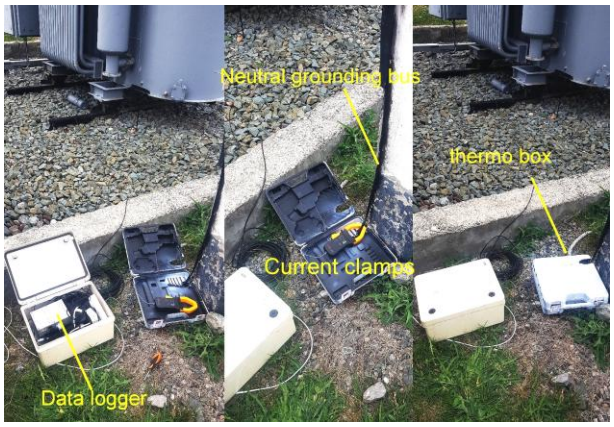

Figure 4. Current sensor on the grounding bus of the 2.5 MVA power transformer at the Ininskaya power substation

Note that installing the current sensor in other substations faced significant difficulties because their transformers had a higher capacity and hence a more complex grounding that usually comprises several buses. Putting the sensor in only one bus leads to a decrease in the detected current. For reasons of accuracy, it would be desirable to install the sensor in a bus directly connecting the grounding knife to the transformer, but substation personnel raise objections to this variant.

It must also be considered that the Ininskaya power substation is located 4 km from the Ininskaya SPP, whose power transformer's external winding is also grounded. Therefore, the current I_{0PS}, which is only a certain part of the geomagnetically induced current I_0, passes through the grounding of the Ininskaya power substation. Their ratio depends on the ratio between resistances of primary windings of power transformers of the substation and the solar power plant and their groundings:

$$1/\beta = \frac{I_{0PS}}{I_0} = \frac{1}{1+\dfrac{R_1+R_{g1}}{R_2+R_{g2}}} = \frac{R_2+R_{g2}}{R_1+R_{g1}+R_2+R_{g2}}. \quad (3)$$

Here, R_1, R_2 and R_{g1}, R_{g2} are resistances of primary phase windings of power transformers and groundings at the Ininskaya power substation and the Ininskaya SPP respectively. At R_1=7.1 Ω, R_2=0.42 Ω, R_{g1}=R_{g2}=2 Ω, we get $1/\beta_0 = 0.210 = 1/4.77$.

Since the power consumed by the village is low, only one of the two transformers available at the Ininskaya substation is used for power supply, which operate alternately for about a month each. As a result, GIC recording was not continuous — it was not recorded when the transformer T2 was being switched on. Nonetheless, magnetic storms were observed on April, 16, April 19, April 26, May 10–11, June 28, and August 04, 2024 during the recording period. To amass data, E.O. Uchaykin periodically traveled to Inya and collected the measurement results recorded on the flash card.

4. DATA PROCESSING AND RECORDING RESULTS

The measurement results were smoothed by ten values to compensate for the 50 Hz harmonic, which has an amplitude of ~50 mA, and then were cleared of outlying data (all values were removed which were more than 10 SD away from the smoothed curve). Next, using the cleared data, we calculated averages and SDs per second (the latter as a characteristic of the alternating current amplitude in grounding). The dynamics of current and temperature averages per second for April 19, 2024 is depicted in Figure 5. It can be seen that due to the strong dependence of the sensor readings on temperature, which in this case varies by 6° during the day, a daily wave

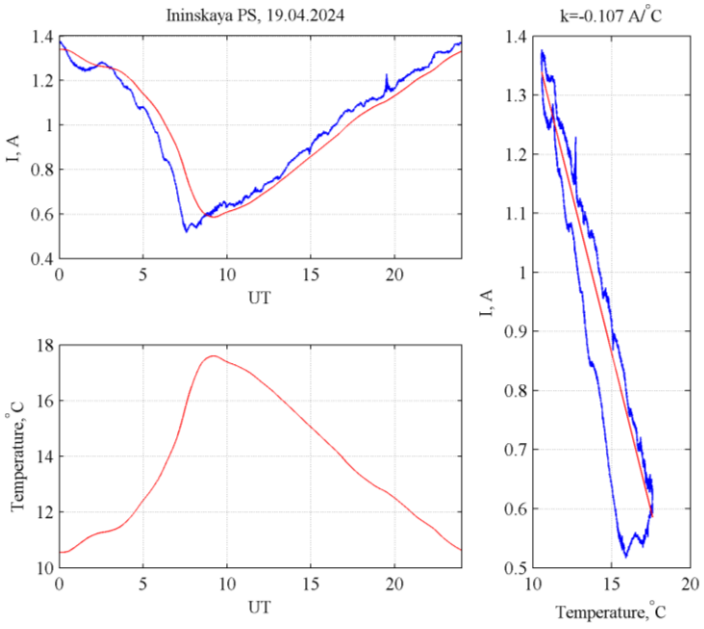

Figure 5. Recording results of current (top left panel) and temperature (bottom left panel) on April 19, 2024. In the top left panel, the measurement results are highlighted in blue; and the theoretical curve calculated from temperature, in red. On the right is the ratio between the recorded current and temperature; the hysteresis of the current-temperature dependence is clearly visible; the red line indicates estimated current-temperature dependence

with ~0.8 A amplitude is observed in the sensor readings. At the same time, as follows from the plot in the right panel, there is a hysteresis in the temperature dependence of the current sensor readings: the wave of the current sensor is somewhat ahead of the daily wave of the temperature sensor readings in phase. This phenomenon is probably caused by the temperature difference at the locations of the temperature sensors and the Hall sensor respectively. Small disturbances with an amplitude to 100 mA are also seen on the current curve, which, in fact, are GICs (on this day there was a magnetic storm with K_p=7). To distinguish them from the background of the temperature wave, it is necessary to balance the temperature dependence. Since the presence of hysteresis greatly complicates such compensation, a short time interval (15 min) was usually taken to isolate GIC, and a second-order polynomial was subtracted from a number of current values for trend compensation. Estimates have shown that the daily temperature wave after such compensation gives corrections of the order of 1 mA. Note that when processing data from the GIC recording system of the Centre of Physical-Technical Problems of Power Energy of the North KSC RAS and the Polar Geophysical Institute the trend was compensated on a daily basis since the zero drift was relatively small due to the active thermal balance of the facility [Barannik et al., 2012]. In our measurements, trend could be compensated over long time intervals (to 8 hrs) only at night when temperature fluctuations were low and relatively regular. In this case, to calculate the trend, a number of measurements were approximated by cubic smoothing splines, using the MATLAB csaps, with a smoothing parameter p=0.01.

The results of the processing at 15-min intervals are presented in Figure 6. Figure 6, *a* shows the SSC event at 22:20 during the August 04, 2024 magnetic storm (according to https://www.obsebre.es/en/variations/rapid); in Figure 6, *b* is the intense bay-like disturbance occurring during the same storm (there was an aurora in Altai at that time). In Figure 6 *a*, *b* (as well as in Figure 6, *c*, *d*), the top panel exhibits variations in the horizontal component H and in the inclination D of the geomagnetic field at the Baigazan magnetic station; the middle panel shows the calculated rates of change of the components dH/dt and dD/dt; and the bottom panel presents the results of GIC measurement at the Ininskaya power substation. It follows from the plots that both events featured field change rates to 2–3 nT/s.

As mentioned above, the observed GIC values should be increased by about an order of magnitude: in this case, in Figure 6, *a* is a maximum current of 0.11 A; and in Figure 6, *b*, 0.37 A. This roughly corresponds to the derived estimates presented in [Uchaikin et al., 2024].

Figure 6, *c* and *d* demonstrates the reaction of GIC to Pc3 and Pc5 geomagnetic pulsations respectively. The bottom panel of Figure 6, *c* clearly shows a current oscillation train caused by geomagnetic pulsations with a period of ~30 s and an amplitude to 1 nT.

There is an obvious strong connection between GIC in the transformer neutral and the geomagnetic pulsations. Note that the geomagnetic field was weakly disturbed at that time: K_p=2+. Thus, weak GICs are generated even by the GMF pulsations that occur every day, but such currents do not have a noticeable effect on the power grid. According to the values at the top of the panels, GIC SD during pulsations is 3–4 times lower than during a substorm. Given that the amplitude of even harmonics (which can be considered as an indicator of the impact on the power grid) in Inya is inversely proportional to the square of the field change rate [Uchaikin, Gvozdarev, 2023], it can be assumed that the effect of these pulsations is by 10–15 dB less.

Of course, these estimates are preliminary since the effect of geomagnetic pulsations on electric networks is still poorly understood. GIC recording systems usually have a time resolution of 1 min, so their data can only be used to study the manifestations of Pc5/Pi3 geomagnetic pulsations in GIC [Yagova et al., 2021]. With a 10 s sampling step between measurements, it becomes possible to examine the effect of Pc4/Pi2 pulsations on GIC [Yagova et al., 2024].

It is interesting to note that at a lower rate of field change dB/dt, Pc5 pulsations (see Figure 6, *d*) have an amplitude comparable to that of Pc3 pulsations (see Figure 6, *c*). This is caused by a greater depth of penetration of the alternating magnetic flux, produced by long-period Pc5 pulsations, into Earth's lithosphere.

The GIC dynamics in the grounding bus of the Ininskaya substation during the onset of the May 10–11, 2024 extreme storm is illustrated in Figure 7. Since the measurements were made at night on May 10, we managed to remove the trend in an 8-hr window. Figure 7 shows that GIC during this storm (which was the severest in the last 20 years) run to 0.138 A. Taking into account the separation of GIC between groundings of the Ininskaya substation and the Ininskaya SPP, the total GIC in both grounding buses could reach 1.3 A, with most of it passing through the grounding of the Ininskaya SPP (which operates at idle speed at night). In addition to this GIC maximum at 22:36 UT, caused by an intense substorm, there is an SSC driven burst of GIC with an amplitude of 92 mA at 17:07 UT.

Table 1 presents the results of processing of data obtained during magnetic storms — maximum measured GICs and standard deviations of measured GIC for three-hour period. It also lists estimated maximum value and SD of total GIC passing through the grounding of the Ininskaya power substation and the Ininskaya SPP. The last column shows the planetary geomagnetic disturbance index K_p, taken from the website of the GFZ Helmholtz Centre for Geosciences [https://kp.gfz-potsdam.de/en/].

5. MODELING GIC IN A HIGH-VOLTAGE POWER GRID OF THE ALTAI REPUBLIC

Gvozdarev et al. [2023] describe a model for calculating GICs in the high-voltage power grid of the Altai Republic, developed on the basis of [Boteler, Pirjola, 2019]. The initial data of the model is data on geomagnetic variations from the Baigazan magnetic station with a discreteness of 1 s.

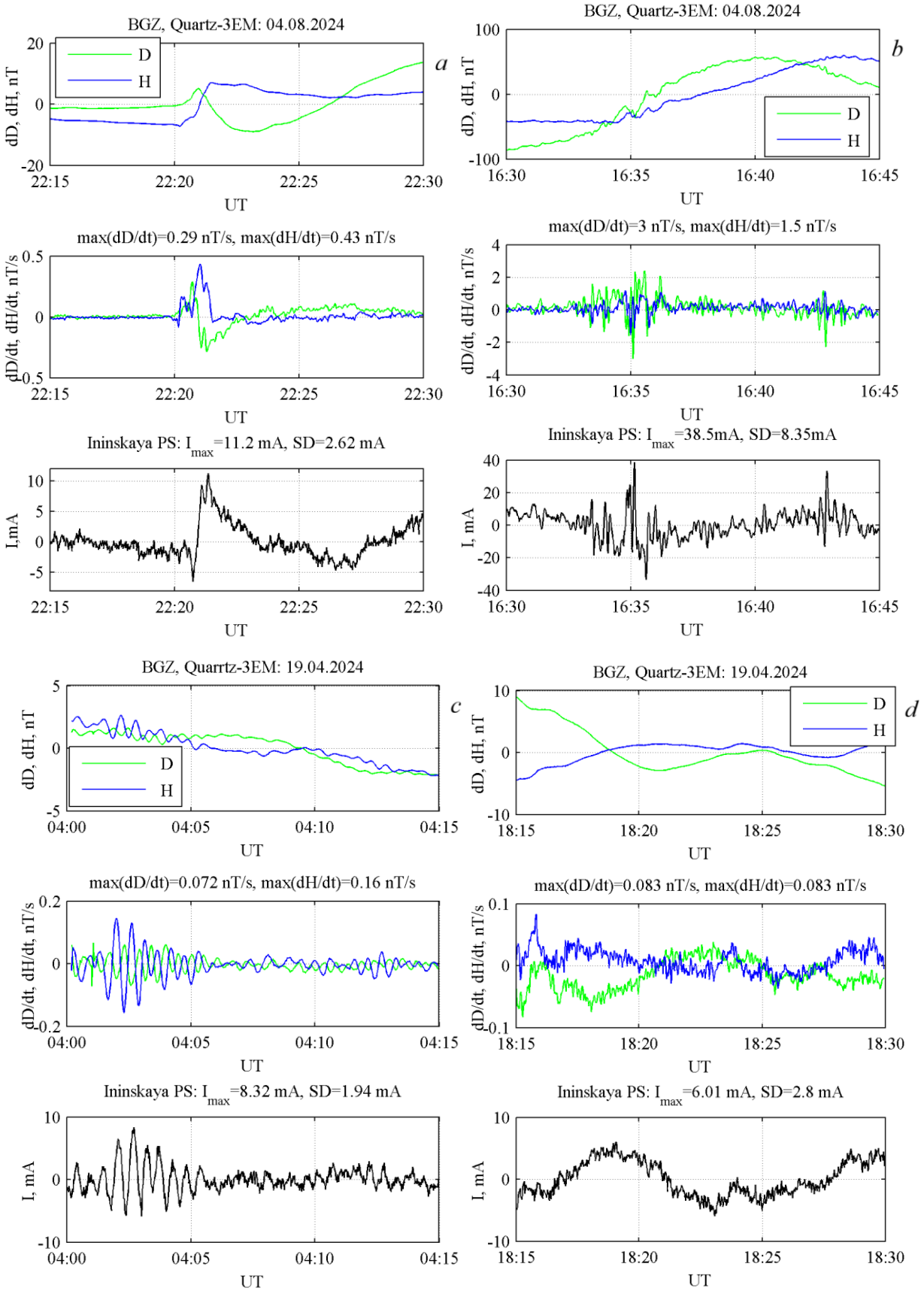

Figure 6. GIC recordings at the Ininskaya substation during SSC (*a*); the onset of an intense bay-like disturbance (*b*); observations of Ps3 (*c*) and Ps5 (*d*) GMF pulsations: top panels present the results of recording of geomagnetic variations at the Baigazan magnetic station; middle panels show the rate of change of field components calculated from the results of recording of geomagnetic variations; bottom panels are GICs recorded at the Ininskaya substation

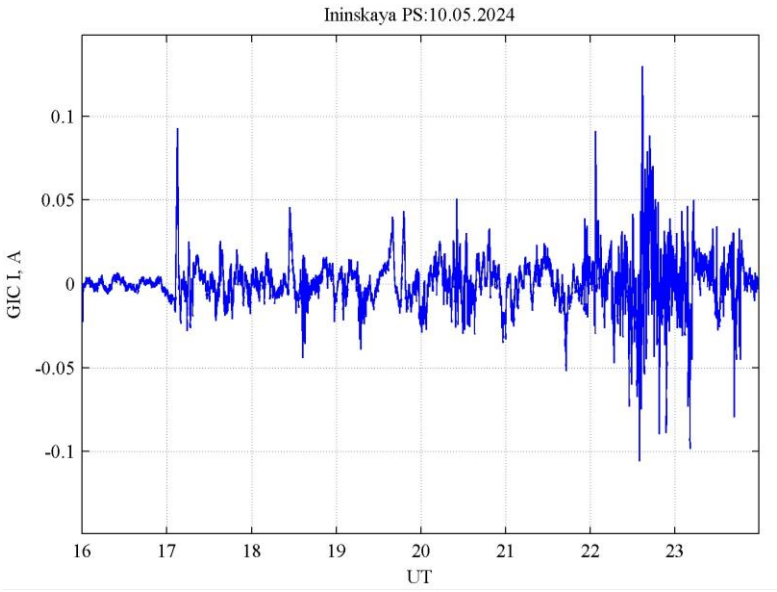

Figure 7. Results of GIC recording at the Ininskaya substation during the May 10, 2024 magnetic storm

Table 1

Maximum measured GICs I and SD of measured GIC in the grounding bus of the Ininskaya substation during magnetic storms, as well as calculated total GICs (βI) for the Ininskaya substation and the Ininskaya SPP

Date	UT	Maximum current, mA		Current SD, mA		K_p
		I	βI	std(I)	std(βI)	
Apr. 16, 2024	15–18	37.2	177	3.13	14.9	5–
	18–21	13.7	65	2.88	13.7	5+
	21–24	11.0	52	2.39	11.4	5
Apr. 19, 2024	12–15	16.8	80	2.22	10.6	5
	15–18	11.2	53	1.94	9.3	6–
	18–21	43.9	209	3.87	18.5	7
Apr. 26, 2024	12–15	13.4	128	3.40	32.4	4
May 10, 2024	15–18	92.5	882	8.15	77.8	8–
	18–21	54.3	518	14.47	138.0	9–
	21–24	137.9	1316	23.51	224.3	9–
May 11, 2024	00–03	No data				9
	03–06	65.2	622	14.30	136.4	8+
	06–09	133.4	1273	25.13	239.7	8+
	09–12	99.8	952	18.39	175.4	9
	12–15	38.7	369	9.17	87.5	9–
June 28, 2024	09–12	32.7	312	5.44	51.9	6
	12–15	15.4	147	2.13	20.3	8–
	15–18	19.4	185	2.22	21.2	6–
	18–21	9.4	90	1.37	13.1	5+
Aug. 04, 2024	12–15	29.8	284	2.40	22.9	7–
	15–18	43.4	414	2.86	27.3	7

Spectra of geomagnetic field horizontal components are calculated from the series of the data: northward $B_y(f)$ and eastward $B_x(f)$. After multiplying by the transfer function $K(f)$, they yield spectra of geoelectric field horizontal components: eastward E_x and northward E_y (to simplify work with geographic coordinates of substations in this case, a geographical, rather than geophysical, coordinate system is used):

$$E_x(f) = K(f)B_y(f), \tag{4.1}$$

$$E_y(f) = -K(f)B_x(f). \tag{4.2}$$

The transfer function is related to the frequency f and the apparent electrical resistivity ρ by the formula

$$K(f) = \sqrt{\frac{i2\pi f\rho}{\mu_0}}, \tag{5}$$

where μ_0 is the magnetic constant.

After the inverse Fourier transform of the geoelectric field spectrum $E_x(f)$, $E_y(f)$, we obtain series of values of these components $E_x(t)$, $E_y(t)$ at different points of time t. From these values we calculate voltages between grounding points of 110 kV PTL:

$$U_{0j}(t) = E_x(t)\left(x_j - x_0\right) + E_y(t)\left(y_j - y_0\right), \quad (6)$$

where x_j, y_j are coordinates of the substations.

The model [Gvozdarev et al., 2023] ignored resistances of primary windings of transformers and their groundings, as well as the dual grounding of 110 kV PTL in Inya and the double-chain design of some PTLs. For the magnetic storms from March to August 2024, GICs were calculated taking these factors into account. An equivalent electrical circuit of the high-voltage power grid is shown in Figure 8. The Altai Republic 110 kV electric grid is made of AS 120/19 wire with linear resistance of 0.249 Ω/km and AZh 120/19 with linear resistance of 0.283 Ω/km. PTLs from Inya to Kosh-Agach and Ulagan are have a double-chain design; the rest, a single-chain design. Information on the length of PTL, the wire types in use, and the transformers installed in the substations was taken from [Scheme and..., 2021] (see Tables 3.3, 3.4 therein); and the electrical parameters of the transformers and PTLs, from the website [https://powersystem.info]. Resistance of subcircuits with regard to transformer resistances is shown in Table 2. When calculating the grounding resistance, it was set to 2 Ω (for Kosh-Agach, 4 Ω due to the presence of permafrost). In Kosh-Agach and Ulagan, it was believed that both transformers were grounded and connected to the 110 kV PTL. In Cherga, one transformer maintains the Ust-Koksa PTL; and the second, the Kosh-Agach PTL. They are galvanically connected at the ground loop level, but their mutual influence was ignored in calculations. At the Ininskaya power substation, only one transformer is connected to PTL

The reactive resistance of the AS 120/19 wire is 0.427 Ω/km at a frequency of 50 Hz; for GIC, this value will be by 3–4 orders of magnitude lower; as a result, for 100 km of the line we will get a resistance of ~0.05 Ω per phase and it can be ignored.

Currents from the three power transmission lines were considered to be summed up in Inya (see Figure 8):

$$I_0 = I_{12} + I_3 = I_1 + I_2 + I_3, \quad (7)$$

where I_0 is the current through the Inya ground node; I_1, I_2, I_3 are currents through the ground nodes in Kosh-Agach, Ulagan, and Cherga respectively; I_{12} is the current through the Inya-Aktash PTL.

It was taken into account that not only the 2.5 MVA power transformer at the Ininskaya power substation, but also the 40 MVA transformer at the Ininskaya SPP were grounded (the resistance of the Inya ground node R_0=1.91 Ω):

$$I_0 = I_{0PS} + I_{0SEP}. \quad (8)$$

Currents in the branches of the equivalent circuit were calculated according to Kirchhoff laws, presented in the matrix form:

$$\begin{pmatrix} R_0 & R_1 & R_{12} & 0 & 0 \\ R_0 & 0 & R_{12} & R_2 & 0 \\ R_0 & 0 & 0 & 0 & R_3 \\ 1 & 0 & -1 & 0 & -1 \\ 0 & -1 & 1 & -1 & 0 \end{pmatrix} \begin{pmatrix} I_0 \\ I_1 \\ I_{12} \\ I_2 \\ I_3 \end{pmatrix} = \begin{pmatrix} U_{01} \\ U_{02} \\ U_{03} \\ 0 \\ 0 \end{pmatrix}. \quad (9)$$

Here R_0, R_1, R_{12}, R_2, R_3 are resistances of subcircuits (shown in Table 1); I_0, I_1, I_{12}, I_2, I_3 are currents in them; U_{01}, U_{02}, U_{03} are voltages between Inya and Kosh-Agach, Ulagan, and Cherga respectively. For each time point, a matrix equation was solved in MATLAB.

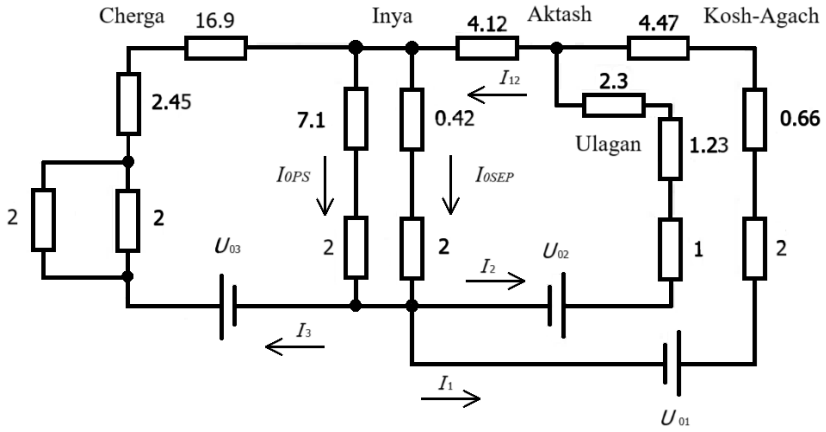

Figure 8. Equivalent circuit of the high-voltage power grid of the southern and central regions of the Altai Republic for calculating GIC

Table 2

Parameters of subcircuits

No.	Subcircuit	Number of circuits in PTL	Length, km	Resistance, Ω		
				PTL	transformers and grounding	total
1	Inya—Aktash R_{12}	2	87.28	4.12		4.12
2	Aktash—Kosh-Agach R_1	2	94.72	4.47	2.66	7.13
3	Aktash—Ulagan R_2	2	55.36	2.30	2.23	4.52
4	Ininskaya—Cherginskaya R_3	1	204.11	16.94	3.45	20.39

The results of comparison between calculations and measurements at the Ininskaya power substation are presented in Figure 9. A qualitative agreement is seen between the calculation and the measurements. The differences between the model and the measurements may be caused by a mismatch between the real transfer function, in which the apparent resistance depends on frequency [Pospeeva et al., 2014], and the model one.

Gvozdarev et al. [2023] chose ρ=500 Ω·m for the apparent electrical resistivity, which is intermediate between the value of this parameter for mountain basins filled with quaternary sediments and their mountain framing in Southeastern Altai [Pospeeva et al., 2014]. The model assumes the approximation of the homogeneous conductivity of the Earth's crust in Altai as the simplest. In reality, there is both a lateral difference in resistivity between intermountain basins and their mountain framing, complicated by the presence of well-conducting fault zones (to 2 Ω·m), and a decrease in resistance with depth (there is a low-resistance crust layer in Altai). The apparent resistivity is shown to decrease by an order of magnitude with a decrease in frequency from 1 Hz to 0.01 Hz [Pospeeva et al., 2014]. Moreover, permafrost, whose thickness reaches 50 m in the mountainous Kosh-Agach region, can make its contribution.

Note that the agreement of the measurement results with the model significantly depends on season, presumably due to changes in the grounding resistance. In April, the best fit between calculations and measurements is observed at a current scaling factor β_0 (see Figure 9, *a*); and in summer, at a scaling factor ~$2\beta_0$ (Figure 9, *b*). This effect was also manifested in the fact that at similar rates of field change on August 4 and April 19 when Pc3 pulsations were observed the GIC amplitude in April (see Figure 6, *c*) was about twice as high.

Grounding in the Ininskaya SPP for a more powerful transformer is of higher quality, and in the summer, when the soil thaws, the grounding resistance in the Ininskaya SPP is significantly lower and hence a smaller fraction of GIC goes through the Ininskaya power substation. Note that the depth of ground freezing in Inya is estimated at 2–3 m, and the effective grounding in the sand-and-shingle deposits of Katun, on which the power substation is placed, is a serious problem.

Table 3 presents the results of model estimates of maximum GICs in Inya, Cherga, and Kosh-Agach during magnetic storms in 2024. It also lists the calculated values of the rate of change of the geomagnetic field horizontal component *dB*/*dt* and the geoelectric field during maxima of calculated GICs in Inya (for April 19, the calculation results are also given for the moment when the measured GIC reached its maximum). The GIC values obtained from measurements at the Ininskaya power substation are shown in parentheses; a scaling factor β_0 was used for the April 16 and 19 storms; and $2\beta_0$, for the rest. The same values were employed to calculate the GIC parameters in Table 1.

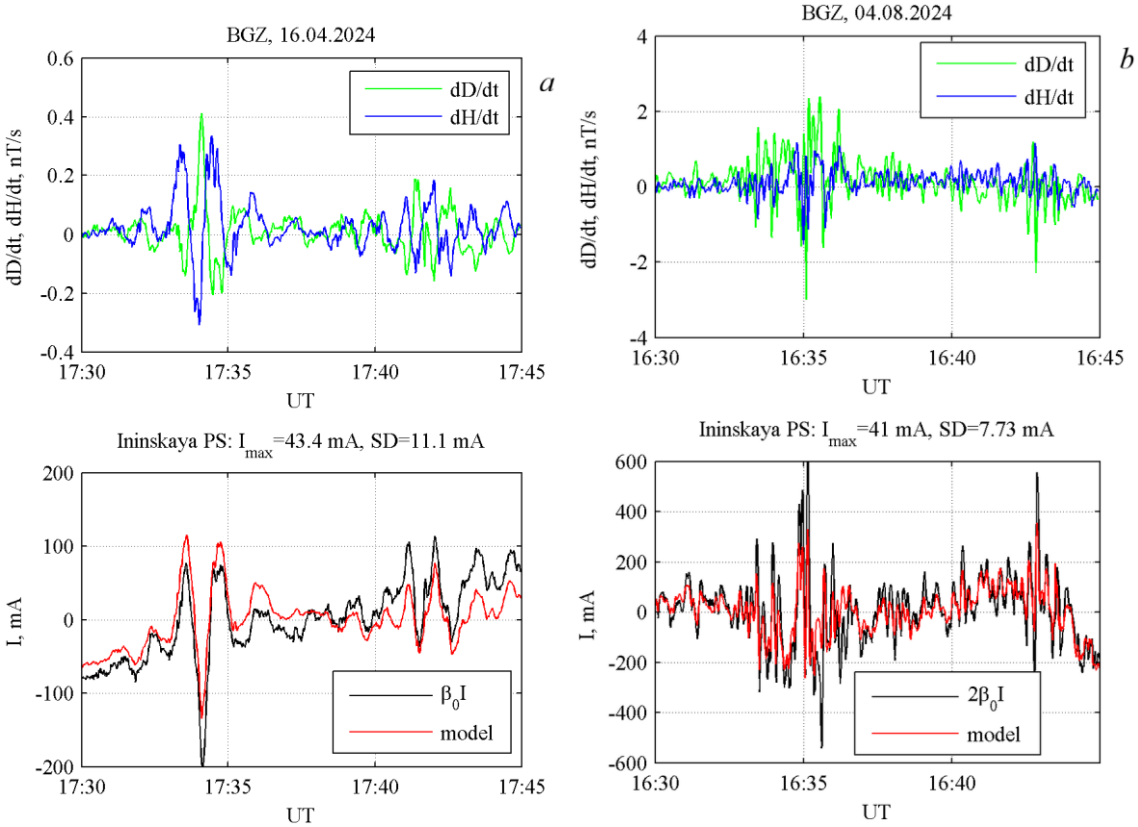

Figure 9. Comparison of GICs measured at the Ininskaya power substation with the results of model calculations on April 16, 2024 (*a*) and August 04, 2024 (*b*): in the top panel is the dynamics of the rate of change of the geomagnetic field components at the Baigazan magnetic station; the bottom panel shows calculated and measured GICs. In April, a conversion factor β_0 is used; in August, $2\beta_0$

Table 3

Estimates according to the model of maximum GIC values in the Altai Republic power grid during magnetic storms in 2024 (experimental GIC values are given in parentheses)

Date	Time of current maximum, UT	Geoelectric field, mV/km	*dB/dt*, nT/min	GIC, mA			
				Inya	Cherga	Kosh-Agach	Ulagan
Mar. 03, 2024	19:34:48	42.8	44.4	400	147	350	197
Mar. 23, 2024	14:10:53	23.4	12.6	214	113	236	91
Mar. 24, 2024	14:37:13	162.0	144.9	1528	711	1551	688
Mar. 25, 2024	04:00:48	89.9	125.1	858	1	302	556
Apr. 16, 2024	20:15:01	19.0	4.8	171(177)	19	33	119
Apr. 19, 2024	14:55:05	25.1	11.6	248(162)	27	125	150
	19:30:41	51.1	40.2	236(371)	262	291	265
Apr. 26, 2024	19:52:23	15.7	5.2	145(104)	11	35	99
May 02, 2024	14:09:23	28.7	13.9	237	165	318	84
May 10, 2024	22:36:43			(1316)			
May 11, 2024	08:20:10			(1273)			
May 13, 2024	10:00:56	40.8	38.0	377	192	406	163
May 16, 2024	07:59:03	45.5	27.7	434	190	424	201
May 17, 2024	13:29:55	23.8	11.2	198	84	187	95
Jun. 07, 2024	14:54:31	45.3	22.6	437	181	411	206
Jun. 28, 2024	11:22:40	72.0	36.8	665(312)	338	716	287
Jul. 26, 2024	03:58:15	48.7	44.9	485	75	278	282
Jul. 30, 2024	05:10:44	37.7	62.6	354	167	363	158
Aug. 01, 2024	04:37:21	37.5	31.8	322	62	25	235
Aug. 04, 2024	16:42:52	61.6	130.1	587(486)	259	576	270
Aug. 11, 2024	09:59:32	51.8	36.8	466	114	367	213
Aug. 12, 2024	08:46:19	120.0	126.0	1163	463	1069	557
Aug. 17, 2024	17:28:10	79.7	35.7	771	312	715	367
Aug. 27, 2024	08:44:01	28.0	12.4	278	84	217	145
Sep. 12, 2024	09:01:26	66.4	72.7	654	224	549	329
Sep. 13, 2024	15:16:09	18.4	18.5	180	13	82	111
Sep. 17, 2024	01:08:53	27.3	28.0	274	63	186	150
Oct. 07, 2024	20:54:31	49.1	33.9	482	41	228	295
Oct. 08, 2024	02:16:46	24.4	18.3	243	37	138	142
Oct. 10, 2024	15:15:58	245.9	227.7	2214	1232	2535	911
Oct. 11, 2024	09:24:04	72.3	39.3	692	576	253	446
Nov. 09, 2024	13:00:14	32.1	40.6	309	128	291	146
Nov. 10, 2024	19:06:18	22.7	7.1	197	35	20	143

According to Table 3, the calculated GIC in Inya exceeded 1 A during the March 24, May 10–11, and August 12 magnetic storms and 2 A (in Kosh-Agach — 2.5 A) during the October 10 storm.

Comparison between the simulation and measurement results shows that they are quite similar for the April storms (April 16, 19, and 26). However, in some cases (June 28, 2024), the model maximum values are higher than the measurement results. One of the reasons may be an underestimation of GIC due to trend subtraction when magnetic variations have a characteristic time longer than 15 min, for example, during bay-like disturbances.

The second possible reason for the discrepancy between the model and the measurements may be the above frequency dependence of the apparent resistivity. Caraballo et al. [2023] have observed that the homogeneous conductivity model yields underestimated GIC values during fast processes as compared to the 1D conductivity model and real measurements. This was explained by a more essential role of the upper part of the geoelectric cross-section in the response to rapid processes. In our case, there is a tendency for the opposite — during sudden commencement of the June 28, 2024 storm and the August 04, 2024 rapid bay-like disturbance, the model gives an overestimated GIC value. Perhaps this is due to the lower resistivity of quaternary sedimentary rocks filling intermountain basins and river valleys, along which PTLs are usually placed, than in the model. The rocks determine the electrical properties of the upper part of the geoelectric cross-section. According to [Novikov, Pospeeva, 2017], for sedimentary rocks of the Kurai and Chuya basins the resistivity ranges from 10 to 300 Ω·m, which is much lower than 500 Ω·m included in the model.

Finally, with lateral heterogeneity, variations in both geomagnetic field horizontal components can affect GIC regardless of PTL orientation [Bedrosian, Love, 2015].

Nevertheless, the results of model calculation can be used to preliminarily estimate the GIC intensity in the region during geomagnetic disturbances. As the measurements accumulate, the model will be refined. In general, the obtained GIC values are lower than the maximum calculated currents for the 115 kV isolated power system in Baja California Sur in Mexico, for which they were estimated at 2 A for a G2 disturbance [Caraballo et al., 2023]. This is likely to be associated with the high

linear resistance of 110 kV PTLs in Russia (0.249 Ω/km in Russia versus 0.061 Ω/km for 115 kV PTL in Mexico) — thus, our 110 kV power grids should be more resistant to GIC.

The results can later be employed to calculate GIC in closely adjacent Siberian 500 kV PTLs. In particular, PTL from the Sayano-Shushenskaya HPP to the Novokuznetsk power substation is at distances not exceeding 300 km from the Baigazan magnetic station, which makes it possible to simulate the dynamics of GIC in it fairly accurately.

CONCLUSION

A system for recording geomagnetically induced currents in the grounding bus of the TMN-2500/110 T1 power transformer has been installed in the Ininskaya power substation in Altai. The Hall current sensor in current clamps has a sensitivity of ~20 mA/V and an error of ~0.5 mA. Recording is performed by a 24-bit ADC 100 times per second. The results are written to an SD card.

Current measurements have a significant temperature trend caused by daily temperature variations (up to 25°C per day in the summer). To isolate GIC, the data is divided into 15-min intervals, at each of which the trend is removed using a second-order polynomial.

GICs were measured during April 16, 2024, April 19, 2024, April 26, 2024, May 10–11, 2024, June 28, 2024, and August 04, 2024 magnetic storms. The May 10–11, 2024 storm was the strongest in the last 20 years, with measured GIC being as strong as 138 mA. It should be considered that GIC in Inya is divided into two unequal parts because transformers are grounded not only at the Ininskaya power substation, but also at the Ininskaya solar power plant. Estimated total GIC in Inya was 1.3 A. The presence of GIC was revealed during observation of Pc3 and Pc5 geomagnetic pulsations.

The results of the GIC measurements have been compared with model calculations in the approximation of homogeneous Earth crust conductivity, using data from the Baigazan magnetic station in Altai. A qualitative agreement was found between the model and calculations. To improve the agreement, it is necessary, on the one hand, to take into account the details of the Altai geoelectric cross-section in the model, and on the other hand, to reduce the temperature sensitivity of current sensors.

GICs during magnetic storms of 2024 were calculated by the model of homogeneous conductivity. The calculated GIC in Inya exceeded 1 A during the March 24, May 10–11, and August 12, 2024 storms, and 2 A during the October 10, 2024 storm.

We have found a seasonal dependence of the GIC intensity at the Ininskaya power substation, presumably caused by redistribution of GIC between the Ininskaya power substation and the Ininskaya SPP due to changes in the grounding resistances in them during soil thawing.

We thank the electricians for maintenance of the Ininskaya power substation, G.P. Voloskov and A.M. Soytoshev, for their support of GIC monitoring at the substation, and A.V. Filatov, Chief Engineer of Gorno-Altaisk Electric Networks, Altai Energo, a branch of Rosseti Siberia Public Joint Stock Company, for his assistance in organizing GIC monitoring in the power grids of the Altai Republic. We are grateful to the inspector of the Altaiskiy Nature Reserve, I.N. Svetloyar, who provided monitoring of geomagnetic variations at the Baygazan cordon, and the administration of the Altaiskiy Nature Reserve, which has been supporting magnetic measurements in the reserve for many years. We express gratitude to the reviewers, whose comments allowed us to significantly improve the article.

The work was financially supported by RSF (Grant No. 23-27-10055) and the Ministry of Education and Science of the Altai Republic.

REFERENCES

Albert D., Schachinger P., Bailey R.L., et al. Analysis of long-term GIC measurements in transformers in Austria. *Space Weather*. 2022, vol. 20, e2021SW002912. DOI: 10.1029/2021SW002912.

Alekseev D., Palshin N., Kuvshinov A. Compilation of 3D global conductivity model of the Earth for space weather applications. *Earth, Planets and Space*. 2015, vol. 67, no. 1, p. 108. DOI: 10.1186/s40623-015-0272-5.

Bailey R.L., Leonhardt R., Möstl C., et al. Forecasting GICs and geoelectric fields from solar wind data using LSTMs: Application in Austria. *Space Weather*. 2022, vol. 20, e2021SW002907. DOI: 10.1029/2021SW002907.

Bakiyanov A.I., Betyov A.A., Gvozdarev A.Yu., Uchaikin E.O. A new magnetical station — Baygazan (Russian Altay, Teletskoe lake). Proc. 6th Science Readings of Y.P. Bulashevich "Deep Structure, Geodynamics, Thermal Field of the Earth, Interpretation of Geophysical Fields"]. Ekaterinburg, 2011, pp. 29–32 (In Russian).

Barannik M.B., Danilin A.N., Kolobov V.V., Selivanov V.N., Kat'kalov Y.V., Sakharov Y.A. A system for recording geomagnetically induced currents in neutrals of power autotransformers. *Instruments and Experimental Techniques*, 2012, vol. 55, iss. 1, pp. 110–115. DOI: 10.1134/S0020441211060121.

Barbosa C.S., Hartmann G.A., Pinheiro K.J. Numerical modeling of geomagnetically induced currents in a Brazilian transmission line. *Adv. Space Res*. 2015, vol. 55, iss. 4, pp. 1168–1179. DOI: 10.1016/j.asr.2014.11.008.

Bedrosian PA, Love J.J. Mapping geoelectric fields during magnetic storms: Synthetic analysis of empirical United States impedances. *Geophys. Res. Lett*. 2015, vol. 42, pp. 10160–10170. DOI: 10.1002/2015GL066636.

Bolduc L. GIC observations and studies in the Hydro-Québec power system. *J. Atmos. and Solar-Terr. Phys*. 2002, vol. 64, pp. 1793–1802. DOI: 10.1016/S1364-6826(02)00128-1.

Boteler D.H., Pirjola R.J. Numerical calculation of geoelectric fields that affect critical infrastructure. *Intern. J. Geosciences*. 2019, vol. 10, pp. 930–949. DOI: 10.4236/ijg.2019.1010053.

Caraballo R., González-Esparza J.A., Pacheco C.R., Corona-Romero P. Improved model for GIC calculation in the Mexican power grid. *Space Weather*. 2023, vol. 21, no.1, e2022SW003202. DOI: 10.1029/2022SW003202R.

Espinosa K.V., Padilha A.L., Alves L.R., et al. Estimating geomagnetically induced currents in southern Brazil using 3D Earth resistivity model. *Space Weather*. 2023, vol. 21, e2022SW003166. DOI: 10.1029/2022SW003166.

Gaunt C.T., Coetzee G. Transformer failures in regions incorrectly considered to have low GIC-risk. *2007 IEEE Lausanne Power Tech*. Lausanne, Switzerland, 2007, pp. 807–812. DOI: 10.1109/PCT.2007.4538419.

Gil A., Berendt-Marchel M., Modzelewska R., et al. Review of geomagnetically induced current proxies in mid-latitude European countries. *Energies*. 2023, vol. 16, p. 7406. DOI: 10.3390/en16217406.

Gusev Yu.P., Lkhamdongdog A.D., Monakov Yu.V., Yagova N.V. Sign-constant current influence on flux linkage balance of power transformer's primary and secondary winding *Releinaya zashchita i avtomatizatsiya* [Relay Protection and Automation]. 2020, no. 2(39), pp. 20–29. (In Russian).

Gvozdarev A.Yu., Kazantzeva O.V., Uchaikin E.O., Yadagaev E.G. Estimation of geomagnetically induced currents in the Altai republic power system according to the Baygazan magnetic station data. *Bull. Kamchatka Regional Association Educational and Scientific Center (KRASEC). Phys. and Math. Sci.* 2023, vol. 45, no. 4, pp. 190–200. DOI: 10.26117/2079-6641-2023-45-4-190-200.

Hübert J., Beggan C. D., Richardson G.S., et al. Validating a UK geomagnetically induced current model using differential magnetometer measurements. *Space Weather*. 2024, vol. 22, e2023SW003769. DOI: 10.1029/2023SW003769.

Kozyreva O.V., Pilipenko V.A., Dobrovolsky M.N., et al. Database of geomagnetic observations in Russian Arctic and its application for estimates of the space weather impact on technological systems. *Sol.-Terr. Phys.* 2022, vol. 8, iss. 1, pp. 39–50. DOI: 10.12737/stp-81202205.

Mac Manus D.H., Rodger C.J., Dalzell M., Thomson A.W.P., et al. Long-term geomagnetically induced current observations in New Zealand: Earth return corrections and geomagnetic field driver. *Space Weather*. 2017, vol. 15, pp. 1020–1038. DOI: 10.1002/2017SW001635.

Mac Manus D.H., Rodger C.J., Renton A., et al. Implementing geomagnetically induced currents mitigation during the May 2024 "Gannon" G5 storm: Research informed response by the New Zealand power network. *Space Weather*. 2025, vol. 23, e2025SW004388. DOI: 10.1029/2025SW004388.

Marsal S., Torta J.M., Curto J.J., et al. Validating GIC modeling in the Spanish power grid by differential magnetometry. *Space Weather*. 2021, vol. 19, iss. 12. DOI: 10.1029/2021SW002905.

Marshall R.A., Dalzell M., Waters C.L., et al. Geomagnetically induced currents in the New Zealand power network. *Space Weather*. 2013, vol. 10, iss. 8, S08003. DOI: 10.1029/2012SW000806.

Matandirotya E., Cilliers P.J., Van Zyl R.R. Modeling geomagnetically induced currents in the South African power transmission network using the finite element method. *Space Weather*. 2015, vol. 13, pp. 185–195. DOI: 10.1002/2014SW001135.

Matandirotya E., Cilliers, P.J., Van Zyl R.R., et al. Differential magnetometer method applied to measurement of geomagnetically induced currents in Southern African power networks. *Space Weather*. 2016, vol. 14, no. 3, pp. 221–232. DOI: 10.1002/2015SW001289.

Muchini P., Matandirotya E., Mashonjowa E. Analysis of transformer reactive power fluctuations during adverse space weather. *Intern. J. Energy and Power Engineering*. 2024, vol. 18, no. 2, pp. 16–21.

Novikov I.S., Pospeeva E.V. Neotectonics of eastern Gorny Altai: Evidence from magnetotelluric data. *Russian Geology and Geophysics*. 2017, vol. 58, no. 7, pp. 769–777. DOI: 10.1016/j.rgg.2017.06.001.

Parkinson W.D. *Introduction to Geomagnetism — Edinburg*, Scottish Academic Press, 1983.

Pilipenko V.A. Space weather impact on ground-based technological systems. *Sol.-Terr. Phys*. 2021. vol. 7, iss. 3, pp. 68–104. DOI: 10.12737/stp-73202106.

Pospeeva E.V., Vitte L.V., Potapov V.V., Sakharova M.A. Magnetotelleric soundings in the region of recent tectonic and seismic activity (by the example of Gorny Altai). *Geofizika* [Geophysics], 2014, no. 4, pp. 8–16. (In Russian).

Pulkkinen A., Lindahl S., Viljanen A., Pirjola R. Geomagnetic storm of 29–31 October 2003: Geomagnetically induced currents and their relation to problems in the Swedish high-voltage power transmission system. *Space Weather*. 2005, vol. 3, S08C03. DOI: 10.1029/2004SW000123.

Selivanov V.N., Aksenovich T.V., Bilin V.A., et al. Database of geomagnetically induced currents in the main transmission line "Northern transit". *Sol.-Terr. Phys*. 2023, vol. 9, iss. 3, pp. 93–101. DOI: 10.12737/stp-93202311.

Sivokon V.P. A new method for detecting geomagnetically induced currents. *Russian Electrical Engineering*. 2021, vol. 92, no. 11, pp. 685–690. DOI 10.3103/S1068371221110146.

Sokolova O.N., Sakharov Ya.A., Gritsutenko S.S., Korovkin N.V. Utilization-based energy optimization energy storage. *Izvestiya Rossiiskoi Akademii Nauk. Energetika*. [Proc. Russian Academy of Sciences. Power Engineering]. 2019, no. 5, pp. 33–52. (In Russian). DOI: 10.1134/S0002331019050145.

Švanda M., Smičková A., Výbošťoková T. Modelling of geomagnetically induced currents in the Czech transmission grid. *Earth Planets and Space*. 2021, vol. 73, no. 1, p. 229. DOI: 10.1186/s40623-021-01555-5.

Skhema i programma razvitiya elektroenergetiki RA na 2022–2026 [Scheme and development program of the Altai Republic electric power industry for 2022–2026 (approved by the Decree of the Head of the Rep. Altai dated 04/29/2021 No.118-u)]. Gorno-Altaisk: Ministry of Regional Development Altai Republic, 2021. URL: https://docs.cntd.ru/document/574723771 (accessed May 13, 2025). (In Russian).

Taran S., Alipour N., Rokni K., Hosseini S., Shekoofa O., Safari H. Effect of geomagnetic storms on a power network at midlatitudes. *Adv. Space Res.* 2023, vol. 71, iss. 12, pp. 5453–5465. DOI: 10.1016/j.asr.2023.02.027.

Tren'kin A.A., Voevodin S.V., Koblova O.N., et al. Simulating a strong storm impact on Russian interconnected power system of Center. *Electrichestvo* [Electricity]. 2023, no. 2, pp. 37–49. (In Russian).

Trivedi N.B., Vitorello I., Kabata W., Dutra S.L.G., Padilha A.L., Bologna M.S., et al. Geomagnetically induced currents in an electric power transmission system at low latitudes in Brazil: A case study. *Space Weather*. 2007, vol. 5, iss. 4. S04004. DOI: 10.1029/2006SW000282.

Uchaikin E.O., Gvozdarev A.Y. Organization of monitoring of even harmonics amplitudes in the electricity networks of the Altai Republic as an indicator of space weather. *2023 IEEE XVI International Scientific and Technical Conference "Actual Problems of Electronic Instrument Engineering" (APEIE)*. Novosibirsk, 2023, pp. 450–454. DOI: 10.1109/APEIE59731.2023.10347597.

Uchaikin E., Gvozdarev A., Kudryavtsev N. Assessment of the geomagnetically induced currents impact on the power transformers cores of the Altai Republic 110 kV power grid. *E3S Web of Conferences*. 2024, vol. 542, p. 02002. DOI: 10.1051/e3sconf/202454202002.

Uchaikin E.O., Kudin D.V., Gvozdarev A.Yu, Design of induction coil magnetometer based on INT-1 sensor and results of monitoring of magnetical station "Baygazan" *Proc. 14th Young Scientists' Conference "Interaction of Fields and Radiation With Matter"*. Irkutsk, 2015, pp. 267–268. (In Russian).

Uchaikin E., Gvozdarev A., Kudryavtsev N., Yadagaev E.G. On the impact of geomagnetically induced currents on the energy system of the Altai Republic and Siberia. *Russian Electrical Engineering*. 2025. vol. 96, no. 6, pp. 477–484. DOI: 10.3103/S1068371225700622.

Vodyannikov V.V., Gordienko G.I., Nechaev S.A., et al. Geomagnetically induced currents in power lines from data on geomagnetic variations. *Geomagnetism and Aeronomy*. 2006, vol. 46, no. 6, pp. 809–813. DOI: 10.1134/S0016793206060168.

Yagova N.V., Pilipenko V.A., Sakharov Y.A., Selivanov V.N. Spatial scale of geomagnetic Pc5/Pi3 pulsations as a factor of their efficiency in generation of geomagnetically induced currents. *Earth, Planets and Space*. 2021, pp. 73–88. DOI: 10.1186/s40623-021-01407-2.

Yagova N.V., Sakharov Y.A., Pilipenko V.A., Selivanov V.N. Long-period pulsations as an element of space weather influence on technological systems. *Sol.-Terr. Phys.* 2024, vol. 10, iss. 3, pp. 136–146. DOI: 10.12737/stp-103202415.

Watari S., Nakamura S., Ebinara Y. Measurement of geomagnetically induced currents (GIC) around Tokyo. *Earth, Planets and Space.* 2021, vol. 73, p. 102. DOI: 10.1186/s40623-021-01422-3.

Zhang J.J., Wang C., Sun T.R., et al. GIC due to storm sudden commencement in low-latitude high-voltage power network in China: Observation and simulation. *Space Weather*. 2015, vol, 13, pp. 643–655. DOI: 10.1002/2015SW001263.

URL: https://powersystem.info (accessed May 12, 2025).

URL: https://kp.gfz-potsdam.de/en/ (accessed May 12, 2025).

URL: https://obsebre.es/en/variations/rapid (accessed May 12, 2025).

Original Russian version: Gvozdarev A.Yu., Uchaikin E.O., published in Solnechno-zemnaya fizika. 2025, vol. 11, no. 4, pp. 92–105. DOI: 10.12737/szf-114202509. © 2025 INFRA-M Academic Publishing House (Nauchno-Izdatelskii Tsentr INFRA-M).

How to cite this article

Gvozdarev A.Yu., Uchaikin E.O. Experience in monitoring geomagnetically induced currents in the Altai Republic power grid. *Sol.-Terr. Phys*. 2025, vol. 11, iss. 4, pp. 83–96. DOI: 10.12737/stp-114202509.